

doi: 10.18720/MCE.82.14

## Local fuse for improving concentric braces behavior

## Предохранитель по сжимающей нагрузке для улучшения поведения концентрических раскосов

**A. Kachooee\***,  
**M.A. Kafi**,  
**M. Gerami**,  
 Semnan University, Semnan, Iran

**PhD А. Качуй\***,  
**PhD, доцент М.А. Кафя**,  
**PhD, М. Герами**,  
 Университет Семнан, г. Семнан, Иран

**Key words:** local fuse; concentric brace; ductility; energy dissipation capacity; load bearing capacity; steel structure

**Ключевые слова:** местный предохранитель; концентрический раскос; податливость; способность к рассеиванию энергии; грузоподъемность; стальная конструкция

**Abstract.** The concentrically braced system is one of the most common lateral load bearing systems among steel structures. These systems have remarkable lateral stiffness and strength, but their compressive buckling prevents them from being ductile and absorbing optimal energy. In this study to solve this problem, by using numerical and experimental studies, a heuristic method is presented. In this method, a local fuse is used along the rectangular hollow section brace. This fuse is mounted by internal and external auxiliary elements to prevent its local buckling under compressive load. This makes the brace behave in a similar manner in both tensile and compressive cyclic loads, resulting in ductile behavior and high-energy absorption. Also in this study, by using numerical results, an investigation is done for the proper position of the fuse along the braces and its optimal shape.

**Аннотация.** Концентрически стержневая система является одной из наиболее распространенных среди стальных систем с поперечными несущими конструкциями. Эти системы имеют значительную жесткость и устойчивость против поперечной силы, но выпучивание при сжатии ограничивает их податливость и поглощение необходимой энергии. Для решения этой задачи в исследовании используется эвристический метод. В данном методе местный предохранитель используется вдоль прямоугольного полого участка раскоса. Этот предохранитель монтируется внутренними и внешними вспомогательными элементами, чтобы предотвратить его местный изгиб при сжимающей нагрузке. Это приводит к тому, что раскос ведет себя одинаково как при растяжении, так и при сжатии. Результатом является податливость и высокое поглощение энергии. Также, используя численные результаты, проводится исследование правильного положения предохранителя вдоль раскосов и его оптимальной формы.

## 1. Introduction

The concentric braced systems (Figure 1) are one of the most applicable lateral load bearing systems in steel structures. These load bearing systems due to having high stiffness and lateral load bearing with respect to other structural systems have been under focus of attention. The main weakness of these structural systems is global buckling of the bracing under compressive loading. Therefore when these structures undergo a cyclic loading like an earthquake, they exhibit an undesirable ductility with low energy dissipation capacity. In addition, in concentrically braced frames, due to the considerable differences between their tensile and compressive strengths, significant demands are made to beams crossed by braces, columns and beam to column connections, leading to a significant increase in the project's construction costs [1–6]. Hence, researchers from around the world have performed extensive studies to solve this problem in concentric bracings. In continuation, some of these studies are cited.

An off-center bracing system (Figure 2) was introduced [7, 8] for improving of concentrically braced frames (CBF) behavior. It basically consists of the non-straight tension strut with an eccentricity designated as  $e$ . The midpoint is connected to the corner by the third member. Once the load is applied, all these three members are stretched, therefore, act in tension. In the recent decade, extensive research has been conducted on this structural system [9–12]. In one of them [12], some numerical studies have been performed on a frame with off-center bracing system with optimum eccentricity and circular element created. The obtained results revealed that using a ductile element or circular dissipater for increasing the ductility of off-center bracing system and concentric bracing system is useful.

Качуй А., Кафя М.А., Герами М. Предохранитель по сжимающей нагрузке для улучшения поведения концентрических раскосов // Инженерно-строительный журнал. 2018. № 6(82). С. 149–162.

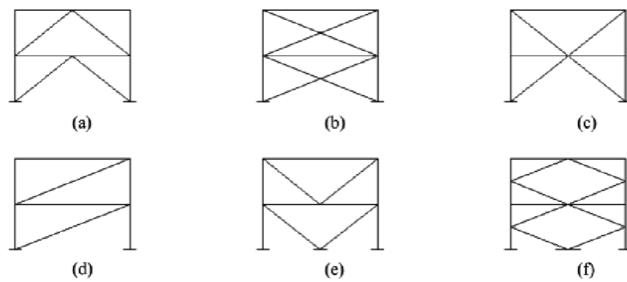


**Figure 1. Different types of concentric braces**

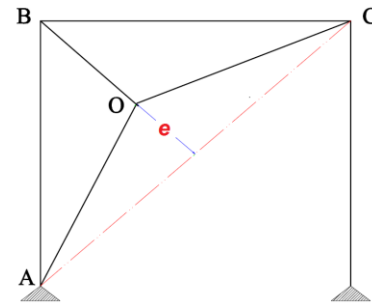


**Figure 2. Off-center bracing system**

As shown in Figure 3a, one of the solutions for enhancing ductility and energy dissipation in concentric braced structures is use of energy dissipation elements located at the intersection of bracings. In this respect application of the rings made of steel tubes as energy dissipater element at intersection with the bracing has been investigated both analytically and experimentally by Abbasnia et al. [13]. The results of these studies have shown that these bracings possess wide and stable hysteresis curves. One of the disadvantages of this system is the certain dimensions of the steel tubes incorporated in the steel rings which cause dimensional restrictions. According to Figure 3b, for this purpose Andalib et al. [14], introduced steel rings made of plates as a replacement for the initial rings and in this respect they have performed an experimental and numerical study to investigate performance of the mentioned rings. The results of Andalib et al. [14] studies exhibit wide and stable hysteresis curves for the rings made of the steel plates.

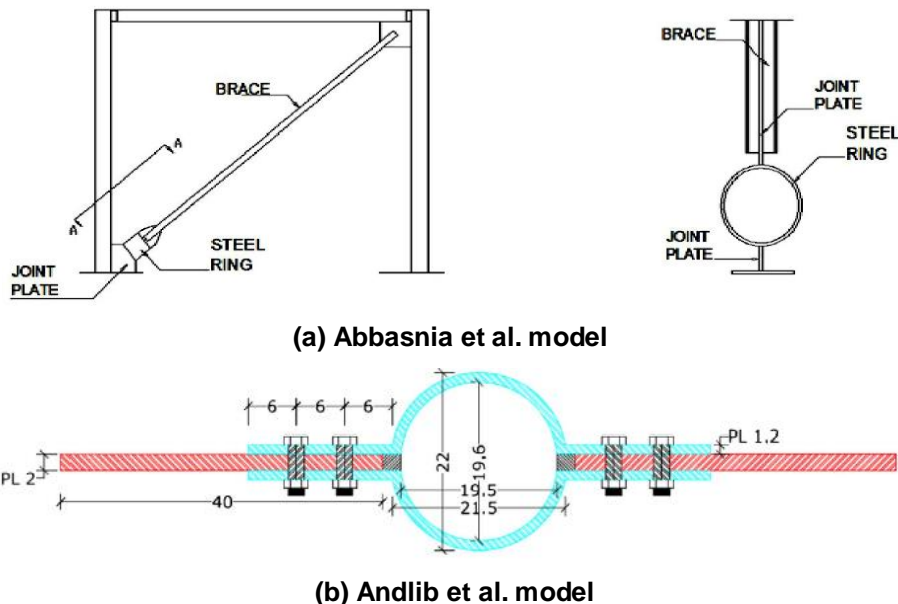


**Figure 3. Brace equipped with circular energy dissipater**

Another method for improving the behavior of the concentric braces is using of fuse in the length of brace [15-18]. A cast modular ductile bracing system (CMDDB) as an alternative for the special CBF structures was introduced [15, 16]. As shown in Figure 4, in these structural systems use has been made of cast component at the middle and ends of the braces. A cruciform cross-section has been utilized for CMDDB because this section increases energy dissipation capacity and low cycle fatigue life and in turn they cause reduced brace failure probability. A system similar to the above system is proposed to replace the conventional concentric braces by Seker et al. [17]. The system uses a three-part steel brace (Figure 5). The idea of this system is to develop an elastic buckling extension of a multi-part column, which includes post-buckling deformations. The results of studies conducted by Seker et al. [17] indicate the consistent and symmetric hysteresis responses of this new concentric brace under cyclic loading. Also, the results of these studies have proven far more energy dissipation capacity than conventional concentric bracing system.

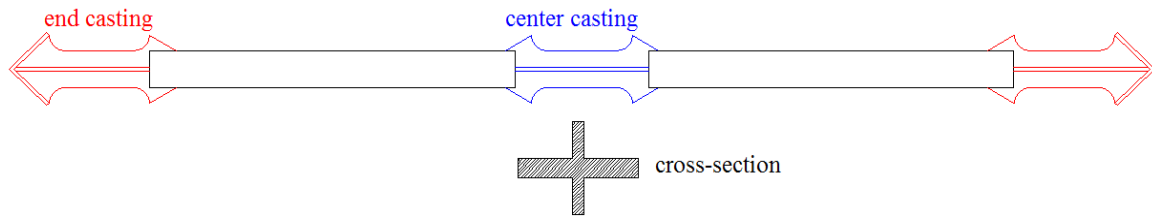


Figure 4. CMDDB model configuration

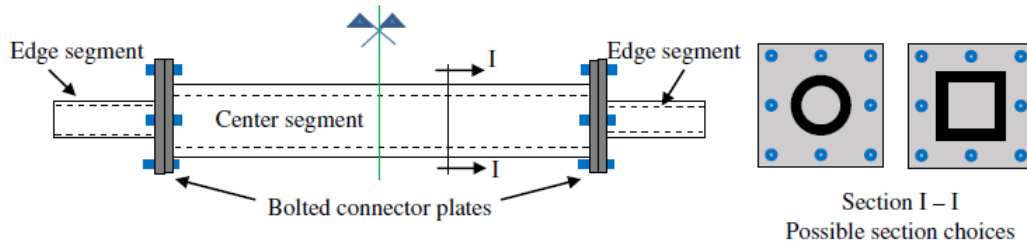


Figure 5. Seker et al. model

Use of two-level or multi-level control systems is another method for improving the seismic behavior of structures which has recently been under focus of attention of researchers. The main idea in these structural systems [19–22], is combination of different control systems with various stiffness and strength values which results into desirable energy absorption in the structure for various earthquake intensities. As shown Figure 6, a system created for implementing the idea of two-level control systems, is the passive tube-in-tube control system. Cheraghi and Zahrai [21] have performed extensive numerical and experimental studies on this structural system. The results of these studies have indicated the extraordinary ductile behavior of this passive structural control system so that the corresponding hysteresis curves of this system have proved its capability in desirable energy absorption under different seismic loading intensities.

According to Figure 7, one of the other invented structural systems for improving seismic performance of the structures with concentric bracings is application of the buckling restrained brace (BRB) [23–27]. In this structural system attempt is made that using bracings which include a casing and core, buckling don't occur in brace [23, 24, 27]. The structures with BRBs present symmetric and stable hysteresis curves which also have significant capacity in terms of ductility and energy dissipation. Furthermore, in the BRB structural system, the non-elastic deformations are entirely and uniformly distributed over the length of BRB and thus damage to other structural elements is prevented.

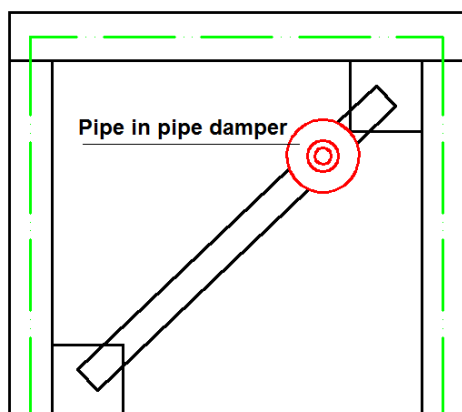


Figure 6. Cheraghi and Zahrai model

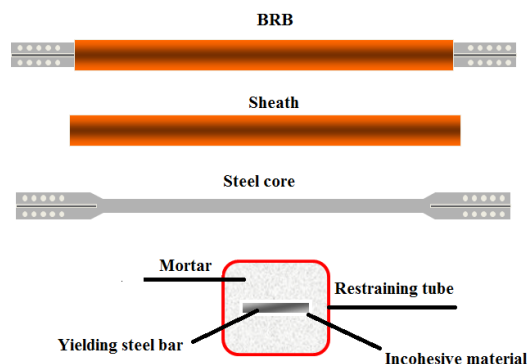


Figure 7. BRB's component

As shown in Figure 8, another method that has been developed as a substitute for conventional concentric braces is all-steel tube-in-tube buckling controlled brace that is called (TinT-BCB) [28–30]. The results of studies conducted by Seker and Shen [28] show that the hysteresis response of this brace was consistent and symmetrical under cyclic loading. The factors affecting the response of these braces include the friction between the two pods, the distance between the internal and external tubes, and the thickness ratio of the inner and outer tubes. Generally in this brace, optimal performance results from a system with smallest gap possible, low friction, and heavier outer tube.

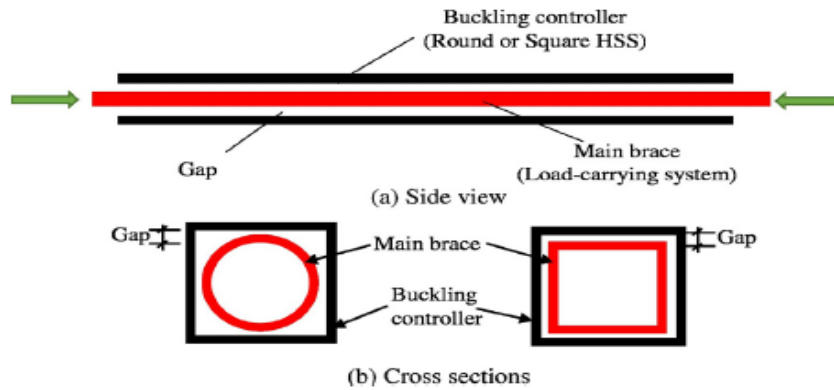


Figure 8. All steel tube in tube BCB

In this research, as shown in Figure 9, a new method is proposed to improve the post buckling behavior of concentric bracings using numerical and laboratory studies. In this method, as Figure 9a, a local fuse (LF) is used along the welded box section brace. This fuse is designed in such a way that the brace buckling occurs locally and in this region. In order to prevent fuse local buckling, internal and external auxiliary elements (AE) are used in this region (Figures 9b and 11b). This causes a symmetrical and stable behavior of the brace under cyclic loading, which results in optimal ductility and a considerable amount of energy dissipation capacity. A complete introduction of the mentioned brace called local fuse auxiliary element concentric brace (LF-AECB) brace is provided in the following. Also a study for determination of the proper position of the fuse along the brace and its optimal shape was done by using numerical studies, in order to obtain the maximum energy dissipation capacity in a LF-AECB brace under cyclic loading. In addition, some different study about LF-AECB is done in [31–33].

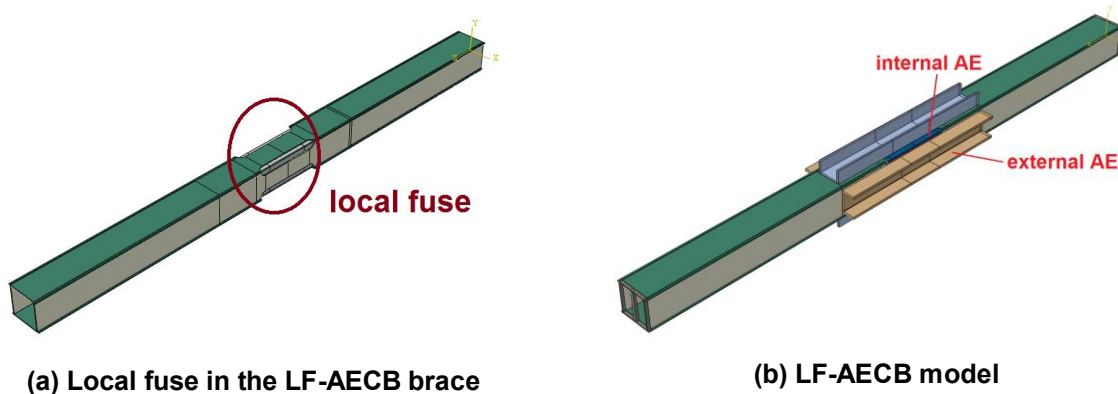


Figure 9. The details of the local fuse auxiliary element concentric braces

## 2. Methods

### 2.1. LF-AECB bracing components

#### 2.1.1. Formulation for calculating fuse area and length

The general pattern of the fuse is shown in Figure 10. As shown in this figure, the local fuse is generated by reducing the cross-section of the brace. In the LF-AECB bracing system, the ultimate load bearing capacity of the brace  $P_{F,brace}$  is equal to the fuse's ultimate load bearing capacity, since the brace cross-section is minimum in this region. According to this fact, the cross-section area of the fuse  $A_{fuse}$  can be calculated from Eq. (1):

$$A_{fuse} \leq \frac{P_{F,brace}}{F_u,brace} \quad (1)$$

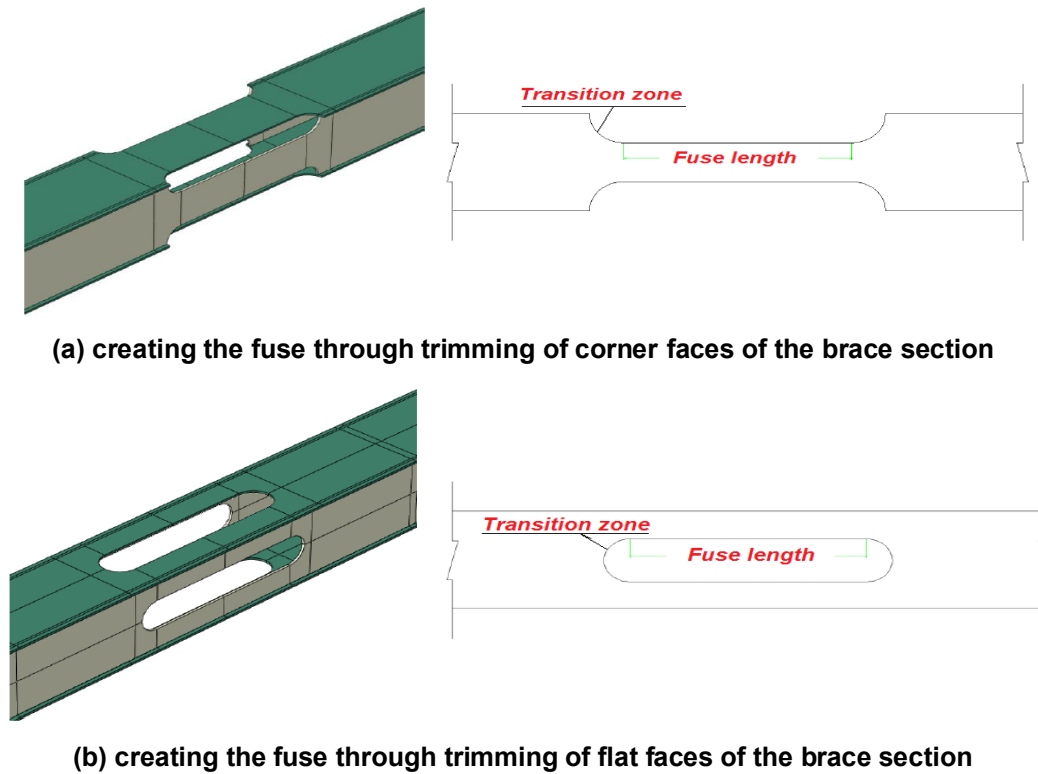


Figure 10. Local fuse in the LF-AECB braces

In the above equation  $F_{u,fuse}$  is the ultimate stress of the fuse material. After calculating the cross-section area of the fuse, the cross-sectional area of the brace,  $A_{brace}$  should be calculated. The basis of the brace cross-sectional design is based on the philosophy that the brace must not totally yield before the fuse reaches the ultimate capacity. The reason is that the overall yielding of the brace causes the material elastic modulus to be substantially reduced, resulting in a general buckling in the brace, which is completely in contradiction with the philosophy of the LF-AECB bracing system. Considering this fact, the calculation of the brace cross-sectional area,  $A_{brace}$  can be obtained from the following equation:

$$A_{fuse} \cdot F_{u,fuse} \leq 0.8 A_{brace} \cdot F_y \quad (2)$$

In the above equation,  $F_y$  is yield stress of the brace material. The presence of 0.8 reduction ratio in Eq. (2) is to ensure that the fuse reaches its ultimate load bearing capacity before the total yield of the brace. Also, the fuse length,  $L_{fuse}$ , should be designed in such a way that the brace buckling occurs locally in this region. Based on this logic, Eq. (3) is formulated to calculate the length of the fuse,  $L_{fuse}$ :

$$L_{fuse} \leq \sqrt{\frac{\pi^2 E I_{min,fuse}}{A_{fuse} \cdot F_{u,fuse}}} \quad (3)$$

In the Eq. (3),  $E$  and  $I_{min,fuse}$  are respectively elastic modulus of fuse material and minimum gyration radius of the weakest part of the fuse.

Also, in order to prevent the stress concentration, a circular transition region is considered in fuse as shown in Figure 10. More information about the above equations is available in [31–33].

### 2.1.2. Auxiliary elements in the LF-AECB bracing

The second component in LF-AECB bracings is the auxiliary element. The auxiliary elements generally include the external and internal areas of the fuse with 1 mm distance from the fuse walls so that they could not affect the fuse load bearing capacity. The philosophy behind existence of the auxiliary element in LF-AECB bracing is to prevent local buckling of the bracing in the fuse area. As is evident from Figure 11, for bracings with box section, auxiliary element is made up of an inner rectangular tube and four outer channels.

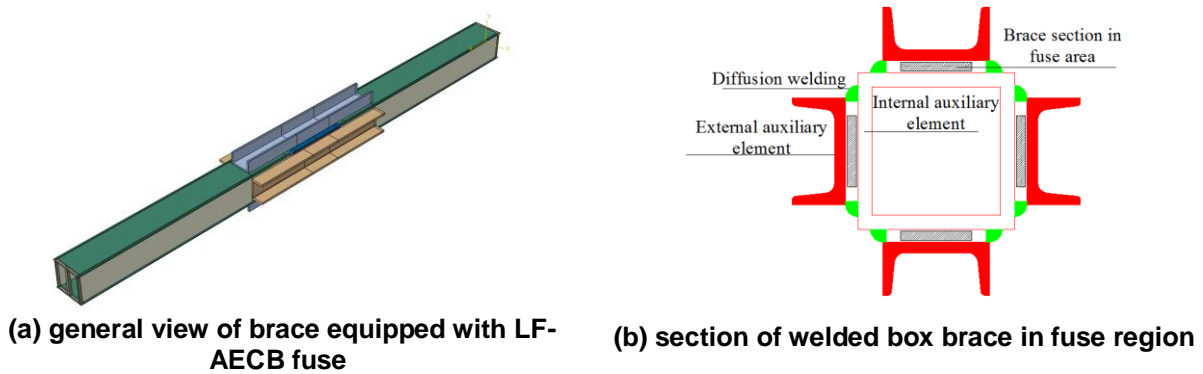


Figure 11. Brace equipped with LF-AECB fuse

The length of these internal and external elements should be at least 15 cm more than the fuse length plus the transition zones. The thickness of these elements must also be selected in such a way that to be able to neutralize the lateral displacement of the fuse. In addition, in order to fix the position of the four external channels, one end of them must be welded to the brace and in the fuse region, as shown in Figure 11b, must be welded to the inner tube throughout both sides of the channels using the diffusion welding. In this way, the position of the inner tube is also fixed.

### 3. Results and Discussion

#### 3.1. Experimental investigation of LF-AECB braces behavior under cyclic loading

##### 3.1.1 Test setup, material properties and loading pattern

In this study, an experimental study was conducted to investigate the behavior of LF-AECB bracing system. In Figure 12, the experimental model and the test setup are shown. According to this figure both ends of the model are welded to the end plates as fixed. The end plates are also connected to a rigid frame on one side using high resistance bolts of 10.9 and a 1000-kN load cell on the other side. In addition, a 2000-kN jack was used to apply load to the model. Also, according to Figure 12, two strain gauges were inserted in the middle distance between the end load plate and the center brace and six LVDTs were also used in different parts of the element. LVDTs 1 and 2 are inserted on the end load plate and LVDTs 3 to 6 are inserted in the middle of the brace.

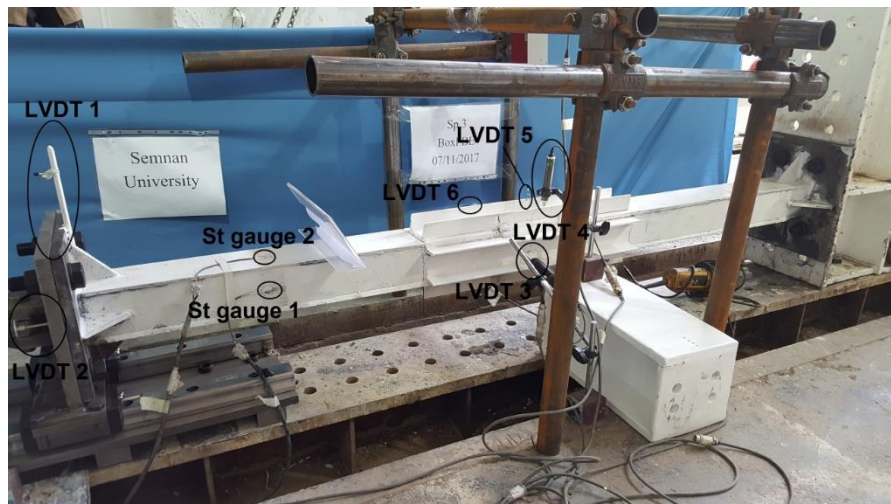


Figure 12. Experiment setup

The brace cross-section and the details of the fuse used, is presented in Figure 13. The fuse has been located in the middle of the brace. Also, as shown in Figure 13b, it has been created by trimming the corners of the brace section. The area of the fuse and its length are considered equal to  $792 \text{ mm}^2$  and 200 mm, respectively, based on Eqs. (2) and (3). The thickness of box section of the brace is 3 mm. According to Figure 11b, in this model, a  $100 \times 100 \times 6$  box is the inner auxiliary element, four standard 60 channels are the external auxiliary elements and the length of all these elements was selected to be 600 mm.

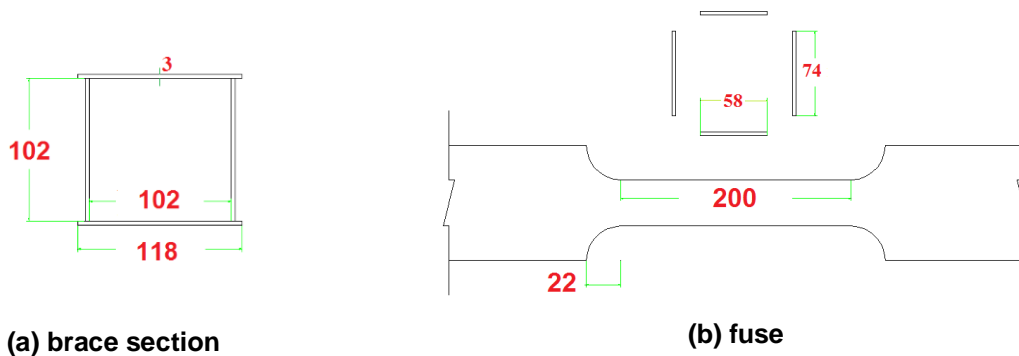


Figure 13. Dimensions of brace section and fuse in experimental models (mm)

The steel that has been used in the experimental model is ST37 and has a specific mechanical characteristic which is presented in Table 1. The mechanical properties of steel materials are obtained using the tensile coupon test shown in Figure 14. In this study, in order to obtain hysteresis responses of the experimental and numerical models, ATC-24 loading pattern [34] is used as shown in Figure 15.

Table 1 Material properties

Material	Yield stress (MPa)	Yield strain	Ultimate stress (MPa)	Ultimate strain	Young's modulus (MPa)	Poisson's ratio
Steel(ST37)	294	0.0025	385	0.1571	117600	0.3



Figure 14. standard tension test of steel material

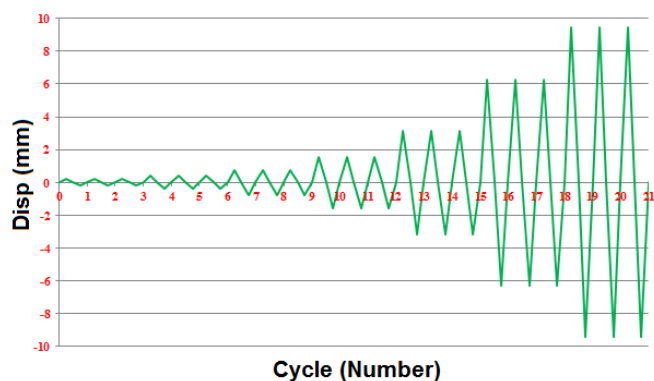


Figure 15. ATC24 load pattern

### 3.1.2. Interpretation of experimental results

In Figure 16, the hysteresis curve obtained from the experimental model is presented. As shown in this figure, the LF-AECB brace has been able to provide a consistent and symmetric behavior under cyclic loading. The tubby and spindle shape curve obtained for this model indicates that the mechanism defined in the LF-AECB bracing system has been able to function correctly and prevent brace buckling. As shown in Figure 16, the studied model does not show any loss of tensile and compressive strength under cyclic loading and with increasing the amount of displacement applied to the brace, the corresponding load bearing capacity has also increased. In this model, as shown in Figure 17a, the internal and external auxiliary elements have succeeded in preventing the fuse from local buckling, so that the brace can continue to operate without loss of strength in compressive load. Finally, in accordance with Figure 17b, in the tensile loading cycle, the brace stopped functioning and a rupture occurred in the end zone of the fuse.

In Figure 18, the experimental model's envelope curve is presented. According to this curve, the studied model in the tensile region has undergone an initial yielding in the fuse region at the displacement of 0.3 mm and the corresponding load of 32.6 kN. In this moment, only, a small part of the fuse has been entered in the plastic region. Also, the maximum load bearing capacity of the model is 251.2 kN, which occurred at the corresponding displacement of 10.2 mm, and after this displacement the model was ruptured in the fuse end zone. In the compressive zone, as well as the tensile zone, the brace offers a good performance. In this zone, the model has undergone an initial yielding at the displacement of 0.33 mm and corresponding load compression of 99.6 kN. Then the brace able to reach a maximum compressive strength of 250.1 kN, which corresponds to a displacement of 9.54 mm. Also ductility ratio for ascending push curve like Figure 18, can be computed from division of ultimate displacement of the model to its

Качуй А., Кафя М.А., Герами М. Предохранитель по сжимающей нагрузке для улучшения поведения концентрических раскосов // Инженерно-строительный журнал. 2018. № 6(82). С. 149–162.

yielding displacement [32, 33, 35]. With respect to the above mentioned issues and according to Eq. 4, the tensile ductility ratio,  $\mu^t$ , and the compressive ductility ratio,  $\mu^c$ , for the experimental model are 34 and 29, respectively. This amount of ductility ratio, especially in the compression zone, is far greater than that of conventional concentric bracings [32, 33], which indicates the more ductile behavior of the LF-AECB bracing systems in comparison to conventional concentric braces.

$$\mu = \frac{\delta_u}{\delta_y} \quad (4)$$

In the Eq. 4  $\mu$ ,  $\delta_y$  and  $\delta_u$ , are the ductility, the yield displacement, and the ultimate displacement of the element, respectively.

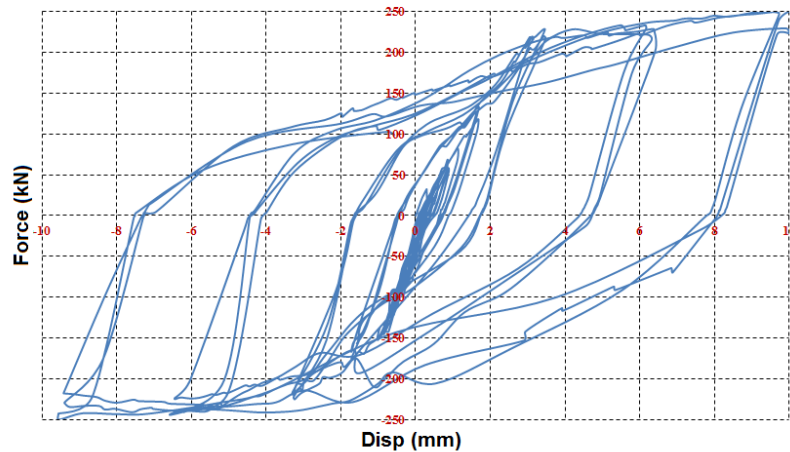


Figure 16. Experimental model hysteresis curve



(a) prevention of fuse local buckling by auxiliary elements



(b) tearing of brace at the end of fuse

Figure 17. Failure of LF-AECB model

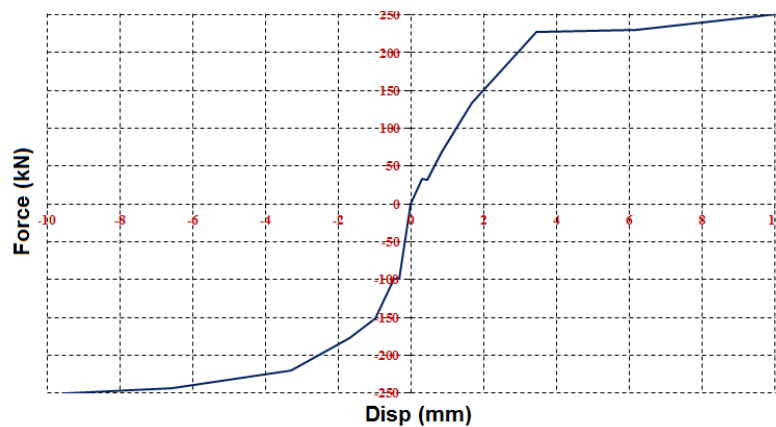


Figure 18. Envelope curve of experimental model

The amount of dissipated energy by the experimental model, which is equal to area under hysteresis curve, was 19728 kNmm. In Figure 19, the relative energy curve, ER (relative energy), of the model is shown. Each point in this curve represents the amount of energy dissipated by the brace in each loading

cycle to the mean of the maximum compressive and tensile displacement corresponding to that cycle. The amount of dissipated energy in each cycle is computed with decreasing the cumulative energy of two sequential cycles. Generally, when the amount of a brace corresponding energy dissipation increases, as the imposed displacement to it increased, then it can be concluded the brace has the optimum energy dissipation capacity. This fact is clearly shown in Figure 19. With respect to this curve, it can be concluded that the LF-AECB braces are able to increase their relative energy dissipation capacity up to their ultimate performance, due to the fact that buckling is not going to occur in them. However, in the case of conventional concentric bracing systems, after the overall buckling, the amount of ER decreases significantly [32, 33].

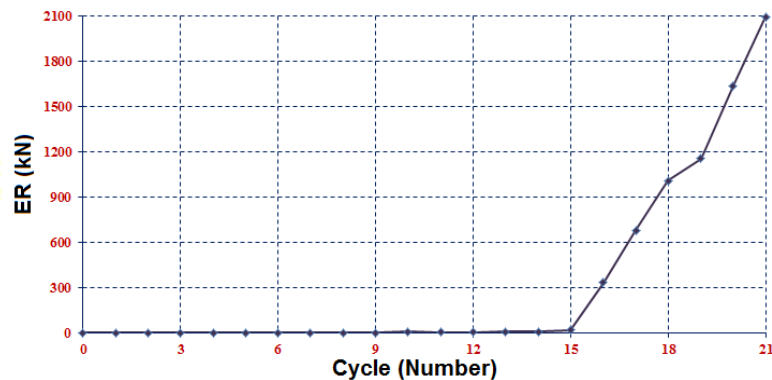


Figure 19. ER curve of experimental model

### 3.2. The effect of local fuse position on the LF-AECB braces behavior

In this section, by using the results of numerical studies, the effect of local fuse position has been investigated on the behavior of LF-AECB bracing systems. First of all, we need to verify the results of numerical studies using the results of experimental studies. For this purpose, according to Figure 11, the Fuse-expr numerical model corresponding to its experimental model in Abaqus 6.12 [36] software was generated. For creating the parts of numerical model in Abaqus software, three dimensional Solid-Deformable elements have been used. In this model, the type of partitioning is Hex and the technique of it is Structured. Also the dimension of elements is equal to 1 cm. Type of elements in numerical model is C3D8I. In other words, the elements are eight point brick with incompatible modes. Also based on Table 1, for modeling the mechanical properties of steel material in Abaqus software, a bilinear stress-strain curve has been used. Then the numerical model was placed under uniform loading. In Figure 20, the push curve of the experimental model and the numerical model capacity curve are compared. As shown in this figure, the numerical model is able to provide a good estimate of the capacity of the experimental model. Also, as seen in the Fig 20, the numerical model has a symmetric capacity curve like experimental model. However, the little differences between two models are possibly related to the differences between real stress-strain curve of steel material of experimental model and bilinear stress-strain curve that has been used in numerical model.

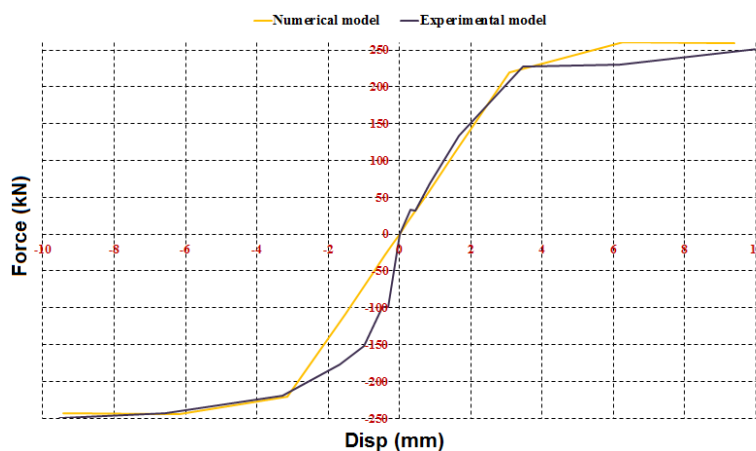
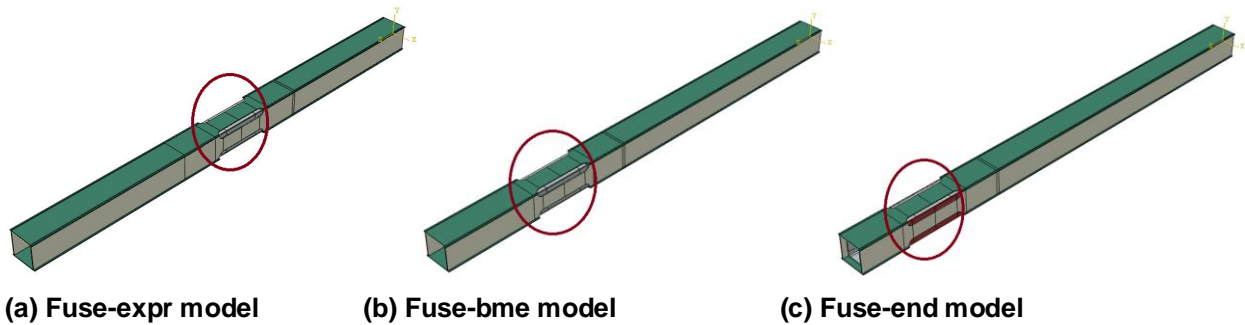


Figure 20. Comparison between envelope curves of experimental model and its corresponding numerical model

In order to determine the effect of local fuse position on the LF-AECB brace behavior, three numerical models were built in Abaqus and then placed under cyclic loading according to Figure 15. These three models are named as Fuse-expr, Fuse-end and Fuse-bme. As shown in Figure 21, in the Fuse-expr model, Качуй А., Кафя М.А., Герами М. Предохранитель по сжимающей нагрузке для улучшения поведения концентрических раскосов // Инженерно-строительный журнал. 2018. № 6(82). С. 149–162.

which is a model corresponding to the experimental model; the fuse is placed in the middle of the brace length and in the Fuse-end and Fuse-bme models fuses are placed at intervals of 200 and 400 mm from the end of the brace, respectively.



**Figure 21 Numerical models for examining of fuse location influence**

In Figure 22, the hysteresis curves of numerical models are compared with each other. As shown in this figure, all three models provide the same behavior under cyclic loading. Also, the maximum tensile load bearing capacity of the models is equal to 260 kN. However, the maximum compressive load bearing capacity of the models varies slightly with each other. In the Fuse-expr model, this was 244 kN, and in the Fuse-bme and Fuse-end models, it was 248 and 246 kN, respectively. In other words, it can be said that the ratio of the lowest to highest values of the maximum load bearing capacity of the models is about 98.5 %, which indicates that these values are extremely close to each other. The amount of dissipated energy the three Fuse-expr, Fuse-bme and Fuse-end models was 19728, 19590, and 19973 kNmm, respectively. The ratio of the maximum amount of energy dissipation between the three models which is related to Fuse-end model, to the minimum value which is related to the Fuse-bme model, is 1.02. This ratio indicates that the fuse position along the brace will not have much effect on the LF-AECB brace energy dissipation capacity.

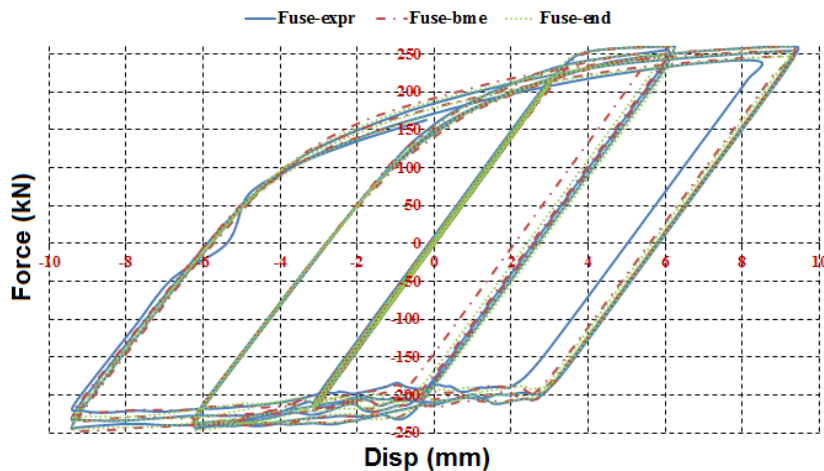
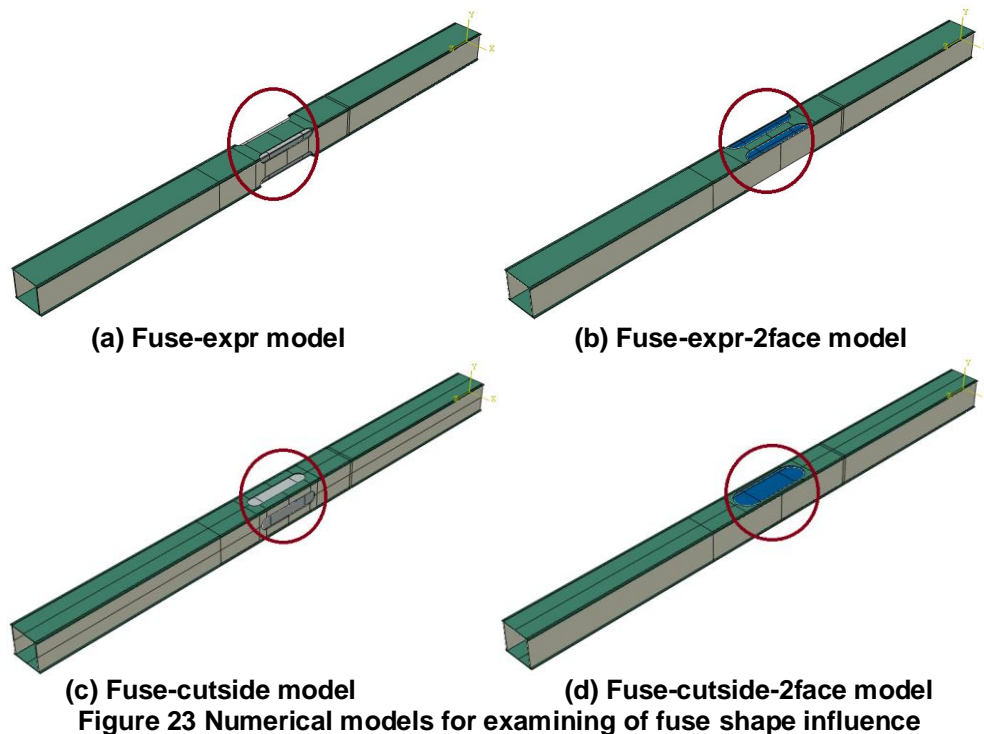


**Figure 22 Comparison between hysteresis curve of numerical models**

In general, and according to the content of this section, it can be concluded that the local fuse position along the brace does not have much effect on the LF-AECB bracing system cyclic response and therefore, depending on the designer opinion and the project execution condition, this element can be installed in any position along the brace.

### 3.3. The effect of the local fuse shape on the LF-AECB bracing cyclic response

This section examines the effect of the fuse shape on the LF-AECB bracing hysteresis response. For this purpose, according to Figure 23, four models have been made in Abaqus 6.12 software. The Fuse-expr model is a model corresponding to the experimental model. In this model, the fuse is created by equally reducing the cross-sectional area on four sides of brace section. Also in this model, the fuse is created by trimming the corner region of the brace sides. In the Fuse-expr-2face model, the fuse is only created on two sides of the brace and by trimming the corner zone of them. In the Fuse-cutside and Fuse-cutside2face models, the fuses are also created by cutting the flat zone of the brace sides, with the difference that in the first model the fuse is distributed equally on four faces of the brace, but in the second model, the fuse is only created on two faces of the brace.



In Figure 24, the hysteresis responses of numerical models are compared. As shown in this figure, the Fuse-cutside and Fuse-expr models, with fuses evenly distributed over their faces, have the most stable and tubby hysteresis curves. The Fuse-cutside model also offers better performance within the two models. The general behavior of numerical models is the same under cyclic loading, but minor differences in load bearing and energy absorption capacities have caused a distinction between them. Fuse-expr model has the greatest maximum tensile load bearing capacity which is equal to 260 kN. The maximum load bearing capacity in the Fuse-cutside model is 258 kN and in two other models it was 252 kN. The greatest maximum load bearing capacity value among the numerical models is only about 3% higher than the smallest of these parameters. With regard to the maximum compressive load bearing capacity, the Fuse-cutside model has the highest value which is equal to 262.5 kN. This parameter in the Fuse-expr, Fuse-expr-2face and Fuse-cutside-2face models has been 243, 232, and 238 kN, respectively. The maximum load bearing capacity of the Fuse-cutside model was 8 %, 13 %, and 10 % higher than the Fuse-expr, Fuse-expr-2face and Fuse-cutside-2face, respectively. Also, the amount of energy dissipated by the Fuse-cutside model is higher compared to other models and it was equal to 21411 kNmm, while this amount for Fuse-expr, Fuse-expr-2face and Fuse-cutside-2face models are equal to 19728, 17474 and 18492 kNmm, respectively. In other words, the Fuse-cutside model has been able to dissipate about 8.5 %, 22.5 % and 16 % more energy than Fuse-expr, Fuse-expr-2face and Fuse-cutside-2face, respectively, under the cyclic loading. Also in the Table 2, the comparison between top models has been presented.

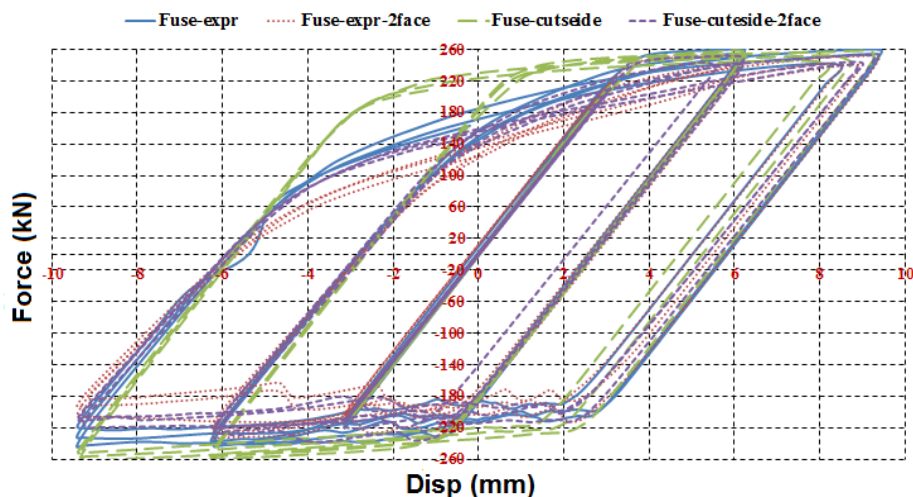


**Table 2 Comparison between numerical models with different fuse shape**

Models	Max tension capacity (kN)	Max compression capacity (kN)	Dissipated energy (kNmm)
Fuse-expr	260	243	19728
Fuse-expr2face	252	232	17747
Fuse-cutside	258	262.5	21411
Fuse-cutside2face	252	238	18492

According to the content presented in this section, it can be concluded that the LF-AECB brace provides its best performance against cyclic loading, when the localized fuse, like Figure 23c, is equally distributed between the bracing faces and has been created by trimming of its flat zone of that faces.

#### 4. Conclusion

In this paper, by using numerical and experimental studies, the new brace system with local fuse has been introduced as an alternative to conventional concentric bracings. The philosophy behind the creation of the LF-AECB braces is to improve the behavior of this element in the compressive zone by preventing the concentric brace from buckling. For this reason, by creating a local fuse in the brace, the overall buckling was prevented in it and the bracing buckling limited locally to this zone. Then, through the use of internal and external auxiliary elements in the fuse region, local buckling was prevented, which resulted in a stable and symmetric cyclic response, and thus, a tubby and spindle shape hysteresis curves was created for this element under cyclic loading. Therefore, the following results are presented in this study:

1. The LF-AECB braces provide a stable and symmetric response to cyclic loading. The reason for this is the use of a restricted lateral fuse mounted on the LF-AECB brace, which prevents brace from buckling and causes the brace to have a well performance in a compressive zone as the tensile zone.
2. The LF-AECB braces, due to the absence of brace buckling, have a very high ductility in the compressive zone, as the tensile zone, while conventional concentric braces have an undesirable ductility due to the brace buckling in the compressive zone, and in many cases the bracing behavior is considered only in the tensile region.
3. The ER curve for the LF-AECB braces is an ascending curve. This means that the amount of energy dissipated in each cycle of displacement loading, increases significantly with displacement increment in the brace, while in conventional concentric braces, the amount of ER after brace buckling is significantly reduced and as a result, full brace capacity will not be used for energy dissipation.
4. According to the numerical studies carried out in this paper, it was concluded that the position of the local fuse along the brace with welded box section does not have much effect on its behavior under cyclic loading, and depending on the project conditions, designer can place the local fuse in any region of the LF-AECB brace.
5. The shape of the local fuse applied to the brace is an effective factor in the LF-AECB brace cyclic response. According to the results of this article, it can be said that the optimal fuse shape for getting the best performance of the LF-AECB brace will be achieved when the fuse is evenly distributed between the brace sides and it is obtained by trimming the internal regions of these faces, like the Fuse-cutside model.

#### References

1. Tremblay, R. Seismic behavior and design of concentrically braced frames. Eng. J. 2001. Vol. 38. Pp. 148–166.
2. Shen, J., Wen, R., Akbas, B., Doran, B., Uckan, E. Seismic demand on brace-intersected beams in two-story X-braced frames. Eng. Struct. 2014. Vol. 76. Pp. 295–312. DOI: 10.1016/j.engstruct.2014.07.022
3. Shen, J., Wen, R., Akbas, B. Mechanisms in two-story X-braced frames. J. Constr. Steel Res. 2015. Vol. 106. Pp. 258–277. DOI: 10.1016/j.jcsr.2014.12.014
4. Uriz, P., Mahin, S.A. Towards earthquake-resistant design of concentrically braced steel-frame structures. PEER Report, College of Engineering, University of California, Berkeley, 2008.
5. Kachooee, A., Kafi, M.A. The Accuracy of Advanced Pushover Analysis Methods in Estimating of Seismic Responses of Steel Moment Frames. 5th national and 1st international conference of steel and structure. Tehran, Iran, 2014.

#### Литература

1. Tremblay R. Seismic behavior and design of concentrically braced frames // Eng. J. 2001. Vol. 38. Pp. 148–166.
2. Shen J., Wen R., Akbas B., Doran B., Uckan E. Seismic demand on brace-intersected beams in two-story X-braced frames // Eng. Struct. 2014. Vol. 76. Pp. 295–312. DOI: 10.1016/j.engstruct.2014.07.022
3. Shen J., Wen R., Akbas B. Mechanisms in two-story X-braced frames // J. Constr. Steel Res. 2015. Vol. 106. Pp. 258–277. DOI: 10.1016/j.jcsr.2014.12.014
4. Uriz P., Mahin S.A. Towards earthquake-resistant design of concentrically braced steel-frame structures. PEER Report, College of Engineering, University of California, Berkeley, 2008.
5. Kachooee A., Kafi M.A. The Accuracy of Advanced Pushover Analysis Methods in Estimating of Seismic Responses of Steel Moment Frames // 5th national and 1st international conference of steel and structure. Tehran, Iran, 2014.

6. Kachooee, A., Kafi, M.A. Effective parameter in panel zone behavior in order to estimate the seismic response of steel moment frame // 5th national and 1st international conference of steel and structure. Tehran, Iran, 2014.
7. Moghaddam, H., Estekanchi, H. On the characteristics of off-centre bracing system. J. Construct. Steel Res. 1995. Vol. 35(3). Pp. 361–376. DOI: 10.1016/0143-974X(94)00050-R
8. Moghaddam, H., Estekanchi, H. Seismic behavior of off-centre bracing systems // J.Construct. Steel Res. 1999. Vol. 51(2). Pp. 177–196. DOI: 10.1016/S0143-974X(99)00007-3
9. Bazzaz, M., Kheyroddin, A., Kafi, M.A., Andalib, Z. Evaluation of the seismic performance of off-centre bracing system with ductile element in steel frames // Steel Compos. Struct., Int. J. 2012. Vol. 12(5). Pp. 445–464. DOI: 10.12989/scs.2012.12.5.445.
10. Bazzaz, M., Kheyroddin, A., Kafi, M.A., Andalib, Z., Esmaili, H. Evaluating the seismic performance of off-centre bracing system with circular element in optimum place. Int. J. Steel Struct. 2014. Vol. 14(2). Pp. 293–304. DOI: 10.1007/s13296-014-2009-x.
11. Bazzaz, M., Andalib, Z., Kafi, M. A., Kheyroddin, A. Evaluating the performance of OBS-C-O in steel frames under monotonic load. Earthq. Struct., Int. J. 2015. Vol. 8(3). Pp. 697–710. DOI: 10.12989/eas.2015.8.3.000
12. Bazzaz, M., Andalib, Z., Kheyroddin, A., Kafi, M.A. Numerical comparison of the seismic performance of steel rings in off-centre bracing system steel rings in off-centre bracing system // Steel Compos. Struct., Int. J. 2015. Vol. 19(4). Pp. 917–937. DOI: 10.12989/scs.2015.19.4.917
13. Abbasnia, R., Vetr, M. G. H., Ahmadi, R., Kafi, M.A. Experimental and analytical investigation on the steel ring ductility. Sharif J. Sci. Technol. 2008. Vol. 52. Pp. 41–48.
14. Andalib, Z., Kafi, M. A., Kheyroddin, A., Bazzaz, M. Experimental investigation of the ductility and performance of steel rings constructed from plates. J. Construct. Steel Res. 2014. Vol. 103. Pp. 77–88. DOI: 10.1016/j.jcsr.2014.07.016.
15. Federico, G., Fleischman, R., Ward, K. Buckling control of cast modular ductile bracing system for seismic-resistant steel frames. J. Construct. Steel Res. 2012. Vol. 71. Pp. 74–82. DOI: 10.1016/j.jcsr.2011.11.010
16. Ward, K.M., Fleischman, R.B., Federico, G. A cast modular bracing system for steel special concentrically braced frames. J. Eng. Struct. 2012. Vol. 45. Pp. 104–116. DOI: 10.1016/j.engstruct.2012.05.025
17. Seker, O., Akbas, B., Seker, P.T., Faytarouni, M., Shen, J. Three-segment steel brace for seismic design of concentrically braced frames. J. Construct. Steel Res. 2017. Vol. 137. Pp. 211–227. DOI: 10.1016/j.jcsr.2017.06.035
18. Legeron, F., Desjardins, E., Ahmed, E. Fuse performance on bracing of concentrically steel braced frames under cyclic loading. J Construct Steel Res. 2014. Vol. 95. Pp. 242–255. DOI: 10.1016/j.jcsr.2013.12.010
19. Balendra, T., Yu, C. H., Lee, F.L. An economical structural system for wind and earthquake loads. J. Eng.Struct. 2001. Vol. 23. Pp. 491–501.
20. Zahrai, S. M., Vosooq, A. K. Study of an innovative two-stage control system: Chevron knee bracing & shear panel in series connection. J. Struct Eng. 2013. Vol. 47(6). Pp. 881–898. DOI: 10.12989/sem.2013.47.6.881
21. Cheraghi, A., Zahrai, S.M. Innovative multi-level control with concentric pipes along brace to reduce seismic response of steel frames. J.Construct. Steel Res. 2016. Vol. 127. Pp. 120–135. DOI: 10.1016/j.jcsr.2016.07.024
22. Simbort E. Selection procedure of seismic-load reduction factor K1 at a given level of ductility factor. Magazine of Civil Engineering. 2012. No. 1(27). Pp. 44–52. DOI: 10.5862/MCE.27.6
23. Sabelli, R., Mahin, S., Chang, C. Seismic demands on steel braced frame buildings with buckling-restrained braces. J.
6. Kachooee A., Kafi M.A. Effective parameter in panel zone behavior in order to estimate the seismic response of steel moment frame // 5th national and 1st international conference of steel and structure. Tehran, Iran, 2014.
7. Moghaddam H., Estekanchi H. On the characteristics of off-centre bracing system // J.Construct. Steel Res. 1995. Vol. 35(3). Pp. 361–376. DOI: 10.1016/0143-974X(94)00050-R
8. Moghaddam H., Estekanchi H. Seismic behavior of off-centre bracing systems // J.Construct. Steel Res. 1999. Vol. 51(2). Pp. 177–196. DOI: 10.1016/S0143-974X(99)00007-3
9. Bazzaz M., Kheyroddin A., Kafi M.A., Andalib Z. Evaluation of the seismic performance of off-centre bracing system with ductile element in steel frames // Steel Compos. Struct., Int. J. 2012. Vol. 12(5). Pp. 445–464. DOI: 10.12989/scs.2012.12.5.445.
10. Bazzaz M., Kheyroddin A., Kafi M.A., Andalib Z., Esmaili H. Evaluating the seismic performance of off-centre bracing system with circular element in optimum place // Int. J. Steel Struct. 2014. Vol. 14(2). Pp. 293–304. DOI: 10.1007/s13296-014-2009-x.
11. Bazzaz M., Andalib Z., Kafi M.A., Kheyroddin A. Evaluating the performance of OBS-C-O in steel frames under monotonic load // Earthq. Struct., Int. J. 2015. Vol. 8(3). Pp. 697–710. DOI: 10.12989/eas.2015.8.3.000
12. Bazzaz M., Andalib Z., Kheyroddin A., Kafi M.A. Numerical comparison of the seismic performance of steel rings in off-centre bracing system steel rings in off-centre bracing system // Steel Compos. Struct., Int. J. 2015. Vol. 19(4). Pp. 917–937. DOI: 10.12989/scs.2015.19.4.917
13. Abbasnia R., Vetr M.G.H., Ahmadi R., Kafi M.A. Experimental and analytical investigation on the steel ring ductility // Sharif J. Sci. Technol. 2008. Vol. 52. Pp. 41–48.
14. Andalib Z., Kafi M.A., Kheyroddin A., Bazzaz M. Experimental investigation of the ductility and performance of steel rings constructed from plates // J.Construct. Steel Res. 2014. Vol. 103. Pp. 77–88. DOI: 10.1016/j.jcsr.2014.07.016.
15. Federico G., Fleischman R., Ward K. Buckling control of cast modular ductile bracing system for seismic-resistant steel frames // J.Construct. Steel Res. 2012. Vol. 71. Pp. 74–82. DOI: 10.1016/j.jcsr.2011.11.010
16. Ward K.M., Fleischman R.B., Federico G. A cast modular bracing system for steel special concentrically braced frames // J. Eng. Struct. 2012. Vol. 45. Pp. 104–116. DOI: 10.1016/j.engstruct.2012.05.025
17. Seker O., Akbas B., Seker P.T., Faytarouni M., Shen J. Three-segment steel brace for seismic design of concentrically braced frames // J.Construct. Steel Res. 2017. Vol. 137. Pp. 211–227. DOI: 10.1016/j.jcsr.2017.06.035
18. Legeron F., Desjardins E., Ahmed E. Fuse performance on bracing of concentrically steel braced frames under cyclic loading // J Construct Steel Res. 2014. Vol. 95. Pp. 242–255. DOI: 10.1016/j.jcsr.2013.12.010
19. Balendra T., Yu C.H., Lee F.L. An economical structural system for wind and earthquake loads // J. Eng.Struct. 2001. Vol. 23. Pp. 491–501.
20. Zahrai S.M., Vosooq A.K. Study of an innovative two-stage control system: Chevron knee bracing & shear panel in series connection // J. Struct Eng. 2013. Vol. 47(6). Pp. 881–898. DOI: 10.12989/sem.2013.47.6.881
21. Cheraghi A., Zahrai S.M. Innovative multi-level control with concentric pipes along brace to reduce seismic response of steel frames // J.Construct. Steel Res. 2016. Vol. 127. Pp. 120–135. DOI: 10.1016/j.jcsr.2016.07.024
22. Симборт Э. Методика выбора коэффициента редукиции сейсмических нагрузок K1 при заданном уровне коэффициента пластичности // Инженерно-строительный журнал. 2012. №1(27). С. 44–52. DOI: 10.5862/MCE.27.6

Качуй А., Кафя М.А., Герами М. Предохранитель по сжимающей нагрузке для улучшения поведения концентрических раскосов // Инженерно-строительный журнал. 2018. № 6(82). С. 149–162.

- Eng Struct. 2003. Vol. 25(5). Pp. 655–666. DOI: 10.1016/S0141-0296(02)00175-X
24. Iwata, M., Kato, T., Wada, A. Buckling-restrained braces as hysteretic dampers. 3rd International Conference STESSA. Montreal, Canada, 2000.
  25. Kiggins, S., Uang, C.M. Reducing residual drift of buckling-restrained braced frames as a dual system. J. Eng. Struct. 2006. Vol. 28(11). Pp. 1525–1532. DOI: 10.1016/j.engstruct.2005.10.023
  26. Maurya, A., Eatherton, M. R., Matsui, R., Florig, S. H. Experimental investigation of miniature buckling restrained braces for use as structural fuses. J. Construct. Steel Res. 2016. Vol. 127. Pp. 54–65. DOI: 10.1016/j.jcsr.2016.07.019
  27. Hoveidae, N., Tremblay, R., Rafezy, B., Davaran, A. Numerical investigation of seismic behavior of short-core all-steel buckling restrained braces. J. Construct. Steel Res. 2015. Vol. 114. Pp. 89–99. DOI: 10.1016/j.jcsr.2015.06.005.
  28. Seker, O., Shen, J. Developing an all-steel buckling controlled brace. J. Construct. Steel Res. 2017. Vol. 131. Pp. 94–109. DOI: 10.1016/j.jcsr.2017.01.006
  29. Momenzadeh, S., Seker, O., Faytarouni, M., Shen, J. Seismic performance of all-steel buckling-controlled braces with various cross-sections. J. Construct. Steel Res. 2017. Vol. 139. Pp. 44–61. DOI: 10.1016/j.jcsr.2017.09.003
  30. Shen, J., Seker, O., Sutchiwcharn, N., Akbas, B. Cyclic behavior of buckling-controlled braces. J. Construct. Steel Res. 2016. Vol. 121. Pp. 110–125. DOI: 10.1016/j.jcsr.2016.01.018
  31. Kachooee, A., Kafi, M. A., Gerami, M. The effect of local fuse on behavior of concentrically braced frame by a numerical study. Civil Engineering Journal. 2018. Vol. 4. Pp. 655–667. DOI:10.28991/cej-0309123.
  32. Kafi, M.A., Kachooee, A. The post buckling behavior of concentrically braced structures. Magazine of Civil Engineering. 2018 No. 2(78). Pp. 16–29. DOI: 10.18720/MCE.78.2.
  33. Kachooee, A., Kafi, M.A. A suggested method for improving post buckling behavior of concentric braces based on experimental and numerical studies. Structures Journal. 2018. Vol. 14. Pp. 333–347. DOI:10.1016/j.istruc.2018.04.003.
  34. ATC24, Guidelines for Cyclic Seismic Testing of Components of Steel Structures, Applied technology council, 1992.
  35. Rakhshanimehr, M., Esfahani, M.R., Kianoush, M.R., Mohammadzadeh, B.A., Mousavi, S.R. Flexural ductility of reinforced concrete beams with lap-spliced bars. Canadian Journal of Civil Engineering. 2014. Vol. 41(7). Pp. 594–604. DOI: 10.1139/cjce-2013-0074
  36. ABAQUS Ver .6.12, User's Manual, RI, USA, 2012.
  23. Sabelli R., Mahin S., Chang C. Seismic demands on steel braced frame buildings with buckling-restrained braces // J. Eng Struct. 2003. Vol. 25(5). Pp. 655–666. DOI: 10.1016/S0141-0296(02)00175-X
  24. Iwata M., Kato T., Wada A. Buckling-restrained braces as hysteretic dampers // 3rd International Conference STESSA. Montreal, Canada, 2000.
  25. Kiggins S., Uang C.M. Reducing residual drift of buckling-restrained braced frames as a dual system // J. Eng. Struct. 2006. Vol. 28(11). Pp. 1525–1532. DOI: 10.1016/j.engstruct.2005.10.023
  26. Maurya A., Eatherton M.R., Matsui R., Florig S.H. Experimental investigation of miniature buckling restrained braces for use as structural fuses // J. Construct. Steel Res. 2016. Vol. 127. Pp. 54–65. DOI: 10.1016/j.jcsr.2016.07.019
  27. Hoveidae N., Tremblay R., Rafezy B., Davaran A. Numerical investigation of seismic behavior of short-core all-steel buckling restrained braces // J. Construct. Steel Res. 2015. Vol. 114. Pp. 89–99. DOI: 10.1016/j.jcsr.2015.06.005.
  28. Seker O., Shen J. Developing an all-steel buckling controlled brace // J. Construct. Steel Res. 2017. Vol. 131. Pp. 94–109. DOI: 10.1016/j.jcsr.2017.01.006
  29. Momenzadeh S., Seker O., Faytarouni M., Shen J. Seismic performance of all-steel buckling-controlled braces with various cross-sections // J. Construct. Steel Res. 2017. Vol. 139. Pp. 44–61. DOI: 10.1016/j.jcsr.2017.09.003
  30. Shen J., Seker O., Sutchiwcharn N., Akbas B. Cyclic behavior of buckling-controlled braces // J. Construct. Steel Res. 2016. Vol. 121. Pp. 110–125. DOI: 10.1016/j.jcsr.2016.01.018
  31. Kachooee A., Kafi M.A., Gerami M. The effect of local fuse on behavior of concentrically braced frame by a numerical study // Civil Engineering Journal. 2018. Vol. 4. Pp. 655–667. DOI:10.28991/cej-0309123.
  32. Кафя М.А., Качуй А. Поведение концентрических раскосов со встроенным предохранителем по сжимающей нагрузке // Инженерно-строительный журнал. 2018. № 2(78). С. 16–29. DOI: 10.18720/MCE.78.2.
  33. Kachooee A., Kafi M.A. A suggested method for improving post buckling behavior of concentric braces based on experimental and numerical studies // Structures Journal. 2018. Vol. 14. Pp. 333–347. DOI:10.1016/j.istruc.2018.04.003.
  34. ATC24, Guidelines for Cyclic Seismic Testing of Components of Steel Structures, Applied technology council, 1992.
  35. Rakhshanimehr M., Esfahani M.R., Kianoush M.R., Mohammadzadeh B.A., Mousavi S.R. Flexural ductility of reinforced concrete beams with lap-spliced bars // Canadian Journal of Civil Engineering. 2014. Vol. 41(7). Pp. 594–604. DOI: 10.1139/cjce-2013-0074
  36. ABAQUS Ver .6.12, User's Manual, RI, USA, 2012.

Ali Kachooee\*,  
00989127910346; ali.kachooee@semnan.ac.ir

Mohammad Ali Kafi,  
00982331533755; mkafi@semnan.ac.ir

Mohsen Gerami,  
00982331533755; mgerami@semnan.ac.ir

Али Качуй\*,  
00989127910346;  
эл. почта: ali.kachooee@semnan.ac.ir

Мохаммад Али Кафя,  
00982331533755;  
эл. почта: mkafi@semnan.ac.ir

Мохсен Герами,  
00982331533755;  
эл. почта: mgerami@semnan.ac.ir

© Kachooee, A., Kafi, M.A., Gerami, M., 2018